

Deliverable 4-2

Computational treatment of light-induced rotary movements in light-fueled molecular components

Gabriele Petraglio, Paolo Raiteri, and Michele Parrinello

*Computational Science, Department of Chemistry and Applied Biosciences ETH Zurich,
USI-Campus, via Giuseppe Buffi 13, 6900 Lugano, Switzerland*

(Dated: September 2, 2005)

I. INTRODUCTION

Molecular machines on the nanoscale represent the new frontier of miniaturization and promise applications in many different fields¹⁻³. These systems are designed to respond to external impulses by producing a mechanical work. Simple examples of molecular switches are for example rotaxanes and catenanes, which are built from mechanically interlocked components. The internal movement can be induced either by chemical (pH), electrical (redox) or optical (photo-excitation) inputs. Even though in solution the type of input is not a major issue, for practical applications on a solid state matrix only electrical or optical inputs are feasible. Since the early publications on electronically configurable molecular-based logic gates⁴ and solid state electronically reconfigurable switches^{5,6} many others have appeared, both for the systems in solution⁷⁻⁹ and in a solid state (on polymer or self-assembled monolayers)¹⁰⁻¹².

In spite of their general importance, theoretical investigation of these compounds began only few years ago and the understanding of the switching mechanisms at atomic level is far from being achieved. Therefore, the main purpose of this deliverable is the development of new theoretical models for a better insight onto these molecular machines. To achieve a good understanding of the process involved the obvious choice would be to perform molecular dynamics (MD) simulations. However, due to the complexity of these systems and to the high activation barriers a time scale problem rises. In fact the switching mechanism occurs on the time scale of milliseconds to minutes, which is not feasible with the today's computer power and techniques to speed up the escape from the energy basins are needed. The standard molecular dynamics is here boosted by a new technique which has been recently developed in our group, *metadynamics*¹³. Metadynamics provides a unified framework for accelerating rare events and computing free energy surfaces (FES). It is based on a dimensional reduction¹⁴ and on a suitable history-dependent potential¹⁵, and requires the preliminary identification of a set of collective variables (CVs) \mathbf{s} , which are functions of the system coordinates, x , and are able to describe the activated process of interest. The dynamics in the space of the chosen CVs is driven by the free energy of the system and is biased by a history-dependent potential, $F_G(\mathbf{s}, t)$, constructed as a sum of Gaussians centered along the trajectory followed by the collective variables up to time t . Metadynamics is a dynamics in the space described by the chosen CVs, and we refer to the point that explores this space

as a *walker*. The method is able optimally to reconstruct the FES and thus, for viable choices of the CVs, allows all the stable and metastable states to be identified. Moreover, at variance with other computational techniques, metadynamics produces atomic trajectories on the free energy surface which allow to identify the real molecular mechanism. Metadynamics has been successfully applied in many different fields, ranging from chemistry^{16–20} to biophysics and ligand docking^{21,22}, material science^{23,24}, crystal structure prediction^{25–27} and systems with discrete degrees of freedom²⁸.

II. IMPROVING METADYNAMICS

In spite of its successes metadynamics shows some limitations for extremely complex systems and improvements are possible. In Ref.²⁹ it was shown that metadynamics is also able to reconstruct a free energy well of a molecular system within a predictable accuracy: $\epsilon \propto \sqrt{\frac{S}{D}}$, where S is the linear dimension of the energy basin and D is the effective diffusion coefficient of the system obtained for example from the typical decay of the velocity auto-correlation function^{30–32}. According to this expression the accuracy of the reconstructed free energy profile is low in the case of small D and large S . Moreover, the filling speed for fixed accuracy decreases as the inverse of the phase space volume to be explored²⁹, thus making accurate reconstruction in more than three dimensions computationally heavy, especially for complex systems such as the ones investigated in this project. We therefore develop a new version of metadynamics which enhances the efficiency, still preserving the accuracy of the method. We implemented a version of the algorithm based on multiple interacting walkers. The power of parallel machines is thus optimally exploited by allowing several walkers to explore simultaneously the same FES.

In a recently submitted paper we extended the analysis of Ref.²⁹ providing an explicit estimate for the error and showing that this implementation is strictly linearly scaling in the number of walkers. The method is intrinsically parallel and can be implemented on loosely coupled clusters since the communication overload, based on the sharing of the walkers' trajectories, is negligible. This enhanced efficiency will make the calculation of FESs in high dimensions more accessible. It is worthy of note that in the multiple walkers metadynamics presented here all the walkers contribute simultaneously to a single combined reconstruction of the FES. This is substantially different from that which is suggested in Ref.¹³ where the

parallelism was invoked only to improve the accuracy with which the force acting on a single walker is calculated.

A substantial speed-up of the reconstruction of the FES is not the only achievement of multiple walkers metadynamics. Indeed, while in theory and very often in practice it has been possible to obtain excellent results with a single walker metadynamics, an important practical problem is to decide when to stop the run. In fact, there could be two problems. During a metadynamics run the relative filling of the basins may oscillate in time. Moreover continuing the metadynamics runs much longer than after the occurrence of the first transition carries the risk of pushing the system outside the basin of interest. This can represent a problem in the case of biological systems, where continuing the metadynamics run may induce important conformational changes, e.g. protein unfolding, which may falsify the FES' reconstruction. While a partial solution to these problems was already introduced in Ref.²², in a recently submitted paper, strictly connected to this deliverable, we show that by combining multiple walkers metadynamics with a weighted histogram analysis technique introduced in Ref.²⁸ we are able to reconstruct complex free energy profiles composed of several basins with complete control over the accuracy.

III. APPLICATIONS

For the present study, we applied the Lagrangian version of metadynamics^{16,21}

$$\mathcal{H} = \mathcal{H}_0 + \frac{1}{2} \sum_{\alpha} M_{\alpha} \dot{s}_{\alpha}^2 - \frac{1}{2} \sum_{\alpha} k_{\alpha} [s_{\alpha}(\mathbf{r}) - s_{\alpha}]^2 + V(t, s_{\alpha}) \quad , \quad (1)$$

where \mathcal{H}_0 is the unperturbed Hamiltonian as used in standard MD and \mathbf{r} are the microscopic coordinates of the system. The second term is the (fictitious) kinetic energy of the collective variables $s_{\alpha}(\mathbf{r})$ and the third one the restraining potential, which couples the collective variables $s_{\alpha}(\mathbf{r})$ to a set of additional dynamic variables s_{α} . The last term

$$V(t, s_{\alpha}) = \sum_{t_i < t} W \exp\left(-\frac{\|s_{\alpha} - s_{\alpha}(t_i)\|^2}{2 \delta s^2}\right) \quad (2)$$

is a history-dependent potential consisting of a series of Gaussians set at discrete time intervals δt . The size of the Gaussians is determined by their width δs and height W . According to the system under investigation we choose different sets of collective variables to describe the switching processes.

A. [2]Catenane

The first system we investigated is the bistable [2]catenane depicted in Fig. 1. It consists of a tetracationic cyclophane, cyclobis(paraquat-*p*-phenylene) ring (CBPQT⁴⁺), mechanically interlocked with a disubstituted crown ether incorporating a tetrathiafulvalene (TTF) and a 1,5-dioxynaphthalene (DNP) unit. This is one of the first bistable molecules being used to produce (solid state) molecular switches, both on Langmuir-Blodgett (LB) and self-assembled monolayers (SAMs)^{5,6,11}. This particular system can exist in two different co-conformers which can be distinguished by the position of the TTF relative to the cyclophane ring. Hereafter we indicate with [A] the co-conformer in which the TTF is located inside the cyclophane and the DNP is outside, while with [B] the one in which the positions of the TTF and of the DNP are exchanged. The ground-state co-conformer for the neutral system is [A⁰]. Experimental and theoretical observations demonstrate that oxidizing [A⁰] to [A⁺] the excess positive charge is located on the TTF and, because of the electrostatic repulsion, a relative rotation of the two rings is induced, see Fig. 1. The rotation ends up when the [B⁺] co-conformer is reached, which is the ground-state for the oxidized system. After a reduction of the system to [B⁰], the ground state [A⁰] is restored by either by relaxation over a barrier or stimulated by a redox cycle of CBPQT⁴⁺, see Fig. 1. In a recent publication Flood et al.⁸ the activation energy for the [B⁰] \longleftrightarrow [A⁰] transformation for many molecular machines has been computed. In particular for the [2]catenane investigated in this study the measured activation barriers are $\Delta G_{298}^{\#} = 16.7$ kcal/mol for the system in solution and $\Delta G_{298}^{\#} = 17.0$ kcal/mol for the system on a polymer matrix.

Scope of our work is to compute the free energy surfaces corresponding to the [B⁺] \longleftrightarrow [A⁺] and [B⁰] \longleftrightarrow [A⁰] switching cycles, to compare the activation barriers with the experimental ones and to provide insight in the atomic behavior during the process.

In the case of the [2]catenane the program used for the simulations was ORAC^{33,34}, a code featuring a multiple time step integration algorithm³⁵. The AMBER force field³⁶ (parm94) and a three-site model for acetonitrile³⁷ were used in the computations. The charges of the [2]catenane were obtained from a restrained fit of the electrostatic potential (RESP)³⁸ calculated on the electronic density by using the Gaussian 98 simulation package³⁹ with the HF/6-31G** basis set. Such charges are assumed to have negligible polarization effects all along the trajectories.

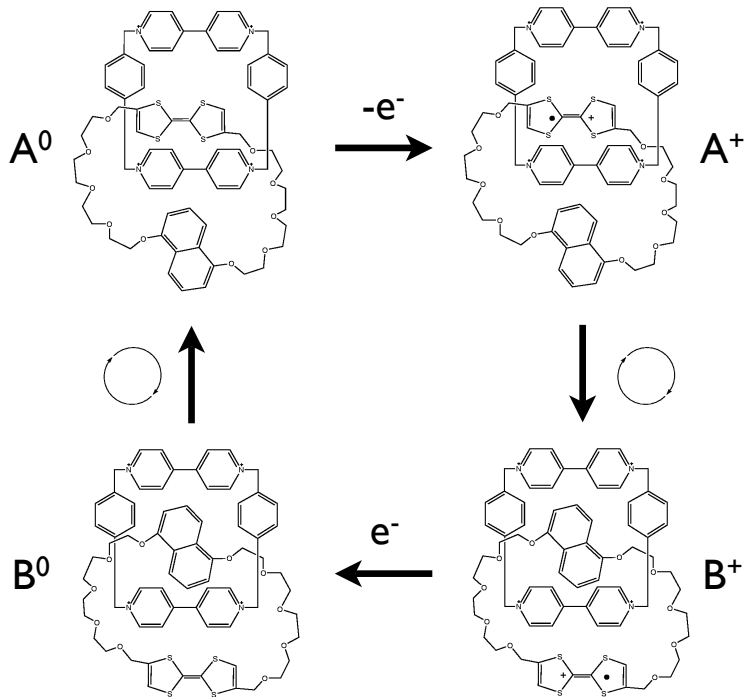


FIG. 1: Switching process of the bistable [2]catenane

1. Electrostatic interactions: Image Boundary Conditions

Since we are studying a charged system, the question of the treatment of the electrostatic interactions and of the boundary conditions is very important. Either one uses standard periodic boundary conditions (PBC) and the Ewald sum⁴⁰ or another possibility is to use explicitly non-periodic boundary conditions. In our case we could have simulated a cubic box big enough to contain both the [2]catenane and its four counterions (hexafluorophosphates) and avoid artifacts deriving from the interactions between replicas; this would be quite time consuming. Another possibility, which has been adopted in this study, is to use intrinsic non-periodic boundary conditions. The solute and some solvent molecules are inserted in a spherical cavity embedded in a dielectric continuum, the effect of which is handled by the method of the images^{41–43}. To each charge in the system (delimited by the surface of the sphere) corresponds an image charge of opposite sign located at a distance corresponding to the reciprocal distance of that charge from the origin of the sphere. This is meant to describe a situation in which the electric charges within a cavity in a dielectric medium polarize the material outside the cavity; this polarization in turn makes a contribution, called the reaction field (RF), to the electric field inside the cavity. We have implemented

and tested our version of the Image Boundary Conditions in the code ORAC, which is used for this project⁴⁴.

2. Results

According to the metadynamics framework the first step to do is the identification of the relevant collective coordinates to describe the switching process. It is immediately evident that a good choice should include a description of the relative position of the two interlocked rings. This can be done by a function named “SCORD” which is zero if the TTF is inside the cyclophane and 0.5 if the DNP is inside the ring. After a few trials we realized that this CV was not sufficient and that something important was missing and by analyzing the trajectories it came out that the solvent degrees of freedom should be accounted for. We therefore added a further CV, the coordination number of the DNP with respect to the solvent molecules.

Given this choice of collective variables we reconstructed the free energy landscape for the $[A^+] \longleftrightarrow [B^+]$ and $[A^0] \longleftrightarrow [B^0]$ switching cycles. We performed various metadynamics runs starting either from the co-conformer $[A]$ or $[B]$.

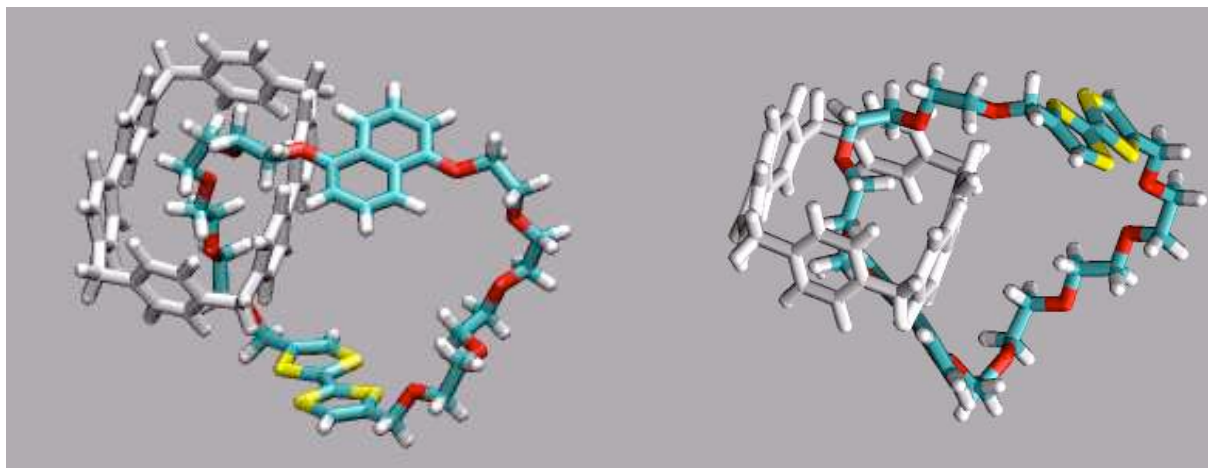


FIG. 2: Two snapshots of intermediates during the switching process. For clarity the solvent molecules are omitted.

The switching mechanism in acetonitrile observed during the metadynamics runs for the $[A^+] \longrightarrow [B^+]$ transition is reminiscent of that observed by Ceccarelli *et al.* (in press, J. Phys. Chem. B) for the same system in vacuum and can be split into three steps. The

first step after the oxidation of the system to $[A^+]$ is the expulsion of the TTF from the cyclophane: in this case the value of the CV SCORD slightly increases, without changing the value of the other CV. During the second step the $\pi - \pi$ interaction between the DNP and the cyclophane breaks up and the crown ether starts rotating around the cyclophane. The last step is the insertion of the DNP into the cyclophane, thus leading to the co-conformer $[B^+]$. In Fig. 2 two snapshots of intermediates during the switching process are shown. Detailed analysis of the inverse rotation does not reveal any significant differences.

Another important feature of metadynamics is its capability of providing the free energy landscape and therefore a direct way of measuring the activation barriers, see Fig. 3. It is worth to underline that the final free energy is almost insensitive to the starting configuration and that, in agreement with the experiments, the $[A^0]$ and the $[B^+]$ co-conformers represent the stable states for the two different oxidation states. In particular $[A^+]$ is 17.5 kcal/mol higher in energy than $[B^+]$ and $[B^0]$ is 14.0 kcal/mol higher than $[A^0]$. We could also determine that the activation barrier for the switching process $[B^+] \rightarrow [A^+]$ is 24 kcal/mol, while for the process $[B^0] \rightarrow [A^0]$ it is 16 kcal/mol. Since both our calculations and the experiments have an accuracy of about 2 kcal/mol the agreement with the experiments is remarkably good.

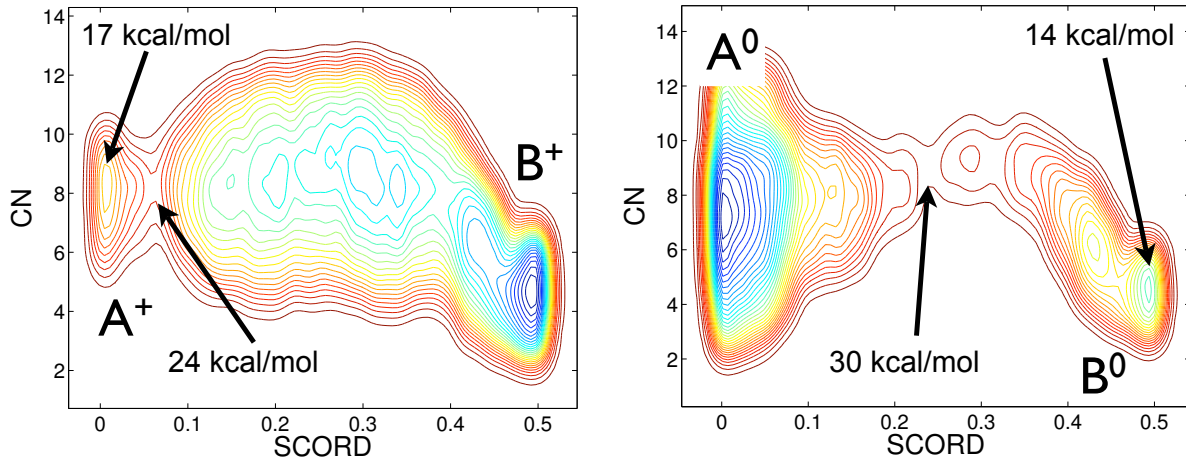


FIG. 3: Free energy surface (FES) of the [2]catenane in solution using SCORD and CN as collective variables. The FESs for the process $[A^+] \leftrightarrow [B^+]$ is shown in the left panel and for the process while that for the process $[A^0] \leftrightarrow [B^0]$ is shown and in the right panel. For convenience the deepest minimum is set to zero energy. The contour lines are plotted each 1 kcal mol^{-1} .

B. [2]Rotaxane

The second system we focus on is a bistable [2]rotaxane which has been well characterized by the group of Prof. Balzani, which is also involved in the BIOMACH project in the group of the University of Bologna. The system is composed of a dumbbell-shaped compound that is encircled by a crown ether which displays a shuttling movement between two charged stations. At equilibrium both are charged (+2), but electrochemical or optical inputs can reduce one of the stations inducing the movement of the ring. Our aim is to compute the energy barriers related to this process and to understand at the atomic level how the movement occurs.

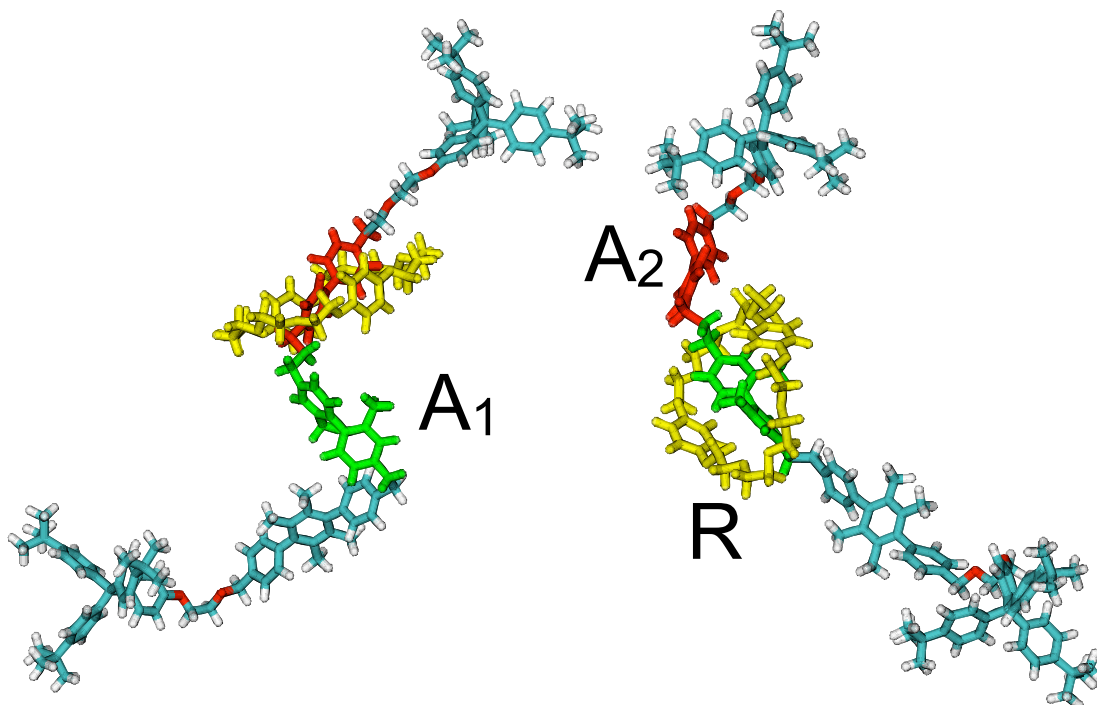


FIG. 4: The two stable co-conformers of the [2]rotaxane. The crown ether is depicted in yellow while the two stations, A_1 and A_2 , are depicted in green and red, respectively. For clarity the solvent molecules are omitted.

The MD simulation are performed with the NAMD code and the AMBER force field. The atomic charges for the rotaxane are obtained by fitting the *ab initio* electrostatic potential with the RESP method. We use a cubic simulation box of about 8 nm in side in which the [2]rotaxane is surrounded by acetonitrile and four hexafluorophosphate (PF_6^-) counterions

to neutralize the system.

A first set of plain MD runs were necessary to obtain an equilibrated configuration and to identify the relevant collective variables. In this simulations we always observed that at equilibrium at least one PF_6^- counterion remains stuck to the rotaxane, irrespectively of the starting configuration. This is against the common belief that the counterions are well separated from the rotaxane. However, since we could not completely exclude this being an artifact due to the small size of our simulation cell, in the metadynamics runs we force the counterions to remain far apart from the rotaxane, postponing a more careful analysis of this point to a later time.

Starting from different initial configurations we could clearly identify the presence of two deep basins of attraction, corresponding to the ring selectively encircling one of the two stations. We also noticed that the ring is highly flexible and that it tends to maximize the number of hydrogen bonds with the two charged stations. Therefore, the collective variables that allow to distinguish in which basin of attraction the system resides are: the position of the ring along the dumbbell and the number of hydrogen bonds formed between the ring and the charged stations. We performed many metadynamics runs using different numbers and combinations of collective variables for the reduced configuration and concluded that at least three are necessary to correctly reproduce the physics of the system. The best choice appears to be the position of the ring along the dumbbell, the number of hydrogen bonds formed with the first station and with the second station, separately. In this case we determined the barriers for this process and the relative depth of the two minima. The barrier for the ring moving from the station with a (+1) charge to that charged (+2) is of 8 kcal/mol and of about 13 kcal/mol for the reverse process but the calculation has not yet fully converged. Both values are slightly smaller than the values suggested by the group of Prof. Balzani, 12 and 14 kcal/mol, respectively. At this point is worth underlying that the estimated accuracy of our values is of about 1.5 kcal/mol and that the role of the counterions is still under investigation. The same calculations for the case in which both the stations are in the (+2) oxidation state are still in progress.

We observed many smooth shuttling processes and could identify the atomic mechanism which can be sketched in three steps. At first the ring breaks the hydrogen bonds with the hosting station assuming a position almost orthogonal with respect to the dumbbell, then it shuttles towards the other station and finally it rotates, re-forming the hydrogen bonds

with the new hosting station.

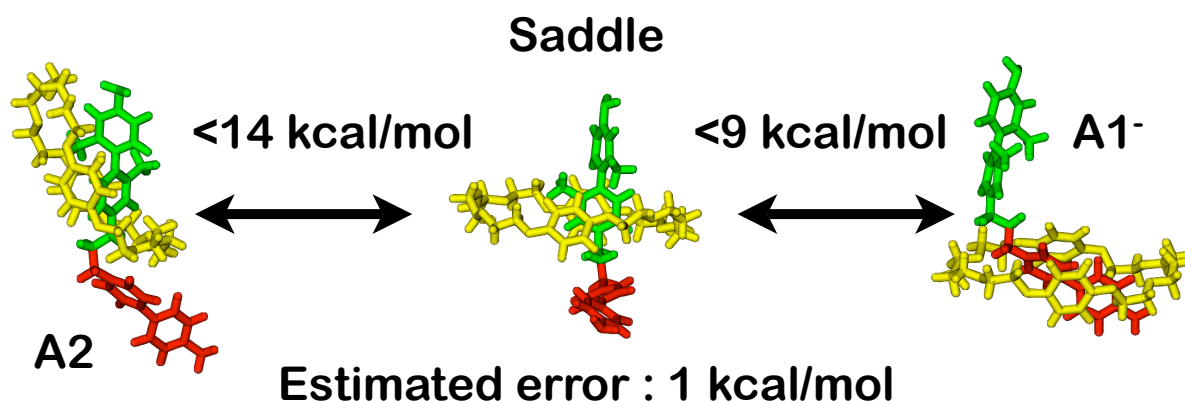


FIG. 5: Atomic mechanism for the shuttling process observed for the reduced [2]rotaxane and the estimated activation barriers. For clarity only the stations and the crown ether are shown.

IV. CONCLUSIONS

In conclusion we have made important steps forward in the construction and mastering of the innovative computational techniques that are needed to simulate complex systems. We have implemented and validated these methodologies, which place our group at the forefront of present day computational research. The agreement between theory and experiments in the case of [2]catenane gives us confidence in the usefulness of our approach. Investigations of the [2]rotaxane are in progress but already very useful results have been obtained.

¹ P. H. Kwan, M. J. MacLachlan, and T. M. Swanger, *J. Am. Chem. Soc.* **126**, 8638 (2004).

² J. D. Badjić, V. Balzani, A. Credi, S. Silvi, and J. F. Stoddart, *Science* **303**, 1845 (2004).

³ Y. Liu, P. A. Bonvallet, S. A. Vignon, B. H. Northrop, H.-R. Tseng, J. O. Jeppesen, T. J. Huang, B. Brough, M. Baller, S. Magonov, et al., *J. Am. Chem. Soc.* **127**, 9745 (2005).

⁴ C. P. Collier, E. W. Wong, M. Belohradský, F. M. Raymo, J. F. Stoddart, P. J. Kuekes, S. R. Williams, and J. R. Heath, *Science* **285**, 391 (1999).

⁵ M. Asakawa, M. Higuchi, G. Mattersteig, T. Nakamura, A. R. Pease, F. M. Raymo, T. Shimizu, and J. F. Stoddart, *Adv. Mater.* **12**, 1099 (2000).

- ⁶ C. P. Collier, G. Mattersteig, E. W. Wong, Y. Luo, K. Beverly, J. Sampaio, F. M. Raymo, J. F. Stoddart, and J. R. Heath, *Science* **289**, 1172 (2000).
- ⁷ M. Venturi, S. Dumas, V. Balzani, J. Cao, and J. F. Stoddart, *New. J. Chem.* **28**, 1032 (2004).
- ⁸ A. H. Flood, A. J. Peters, S. A. Vignon, D. W. Steuerman, H.-R. Tseng, S. Kang, J. R. Heath, and J. F. Stoddart, *Chem. Eur. J.* **10**, 6558 (2004).
- ⁹ J. V. Hernández, E. R. Kay, and D. A. Leigh, *Science* **306**, 1532 (2004).
- ¹⁰ C. P. Collier, J. O. Jeppesen, Y. Luo, J. Perkins, E. W. Wong, J. R. Heath, and J. F. Stoddart, *J. Am. Chem. Soc.* **123**, 12632 (2001).
- ¹¹ M. R. Diehl, D. W. Steuerman, H.-R. Tseng, S. A. Vignon, A. Star, P. C. Celestre, J. F. Stoddart, and J. R. Heath, *ChemPhysChem* **4**, 1335 (2003).
- ¹² H. Yu, Y. Luo, K. Beverly, J. F. Stoddart, H.-S. Tseng, and J. R. Heath, *Angew. Chem. Int. Ed.* **42**, 5706 (2003).
- ¹³ A. Laio and M. Parrinello, *Proc. Natl. Acad. Sci. USA* **99**, 12562 (2002).
- ¹⁴ C. W. Gear, I. G. Kevrekidis, and C. Theodoropoulos, *Comput. Chem. Eng.* **26**, 941 (2002).
- ¹⁵ T. Huber, A. E. Torda, and W. F. van Gunsteren, *J. Comput.-Aided Mol. Des.* **8**, 695 (1994).
- ¹⁶ M. Iannuzzi, A. Laio, and M. Parrinello, *Phys. Rev. Lett.* **90**, 238302 (2003).
- ¹⁷ A. Stirling, M. Iannuzzi, A. Laio, and M. Parrinello, *ChemPhysChem* **5**, 1292 (2004).
- ¹⁸ S. Churakov, M. Iannuzzi, and M. Parrinello, *J. Phys. Chem. B* **108**, 11567 (2004).
- ¹⁹ B. Ensing, A. Laio, F. Gervasio, M. Parrinello, and M. Klein, *J. Am. Chem. Soc.* **126(31)**, 9492 (2004).
- ²⁰ B. Ensing and M. L. Klein, *Proc. Natl. Acad. Sci. USA* **102**, 6755 (2005).
- ²¹ M. Ceccarelli, C. Danelon, A. Laio, and M. Parrinello, *Biophys J.* **87**, 58 (2004).
- ²² F. L. Gervasio, A. Laio, and M. Parrinello, *J. Am. Chem. Soc.* **127**, 2600 (2005).
- ²³ F. Zipoli, M. Bernasconi, and R. Martoňák, *Eur. Phys. J. B* **39**, 41 (2004).
- ²⁴ M. Iannuzzi and M. Parrinello, *Phys. Rev. Lett.* **93**, 025901 (2004).
- ²⁵ R. Martoňák, A. Laio, and M. Parrinello, *Phys. Rev. Lett.* **90**, 75503 (2003).
- ²⁶ P. Raiteri, R. Martoňák, and M. Parrinello, *Angew. Chem. Int. Ed.* **44**, 3769 (2005).
- ²⁷ R. Martoňák, A. Laio, M. Bernasconi, C. Ceriani, P. Raiteri, and M. Parrinello, *Zeitschrift für Kristallographie*, accepted (2005).
- ²⁸ C. Micheletti, A. Laio, and M. Parrinello, *Phys. Rev. Lett.* **92**, 170601 (2004).
- ²⁹ A. Laio, A. Rodriguez-Forteza, F. L. Gervasio, M. Ceccarelli, and M. Parrinello, *J. Phys. Chem.*

- B. **109**, 6714 (2005).
- ³⁰ R. Zwanzig, Phys. Rev. **124**, 983 (1961).
- ³¹ H. Mori, Prog. Theor. Phys. **33**, 423 (1965).
- ³² E. A. Carter and T. J. Heynes, J. Chem. Phys. **94**, 5961 (1991).
- ³³ P. Procacci, T. A. Darden, E. Paci, and M. Marchi, J. Comput. Chem. **18**, 1848 (1997).
- ³⁴ M. Marchi and P. Procacci, J. Chem. Phys. **109**, 5194 (1998).
- ³⁵ M. Tuckerman, B. J. Berne, and G. J. Martyna, J. Chem. Phys. **97**, 1990 (1992).
- ³⁶ W. D. Cornell, P. Cieplak, C. I. Bayly, I. R. Gould, K. M. Merz, Jr., D. M. Ferguson, D. C. Spellmeyer, T. Fox, J. W. Caldwell, and P. A. Kollman, J. Am. Chem. Soc. **117**, 5179 (1995).
- ³⁷ D. M. F. Edwards, P. A. Madden, and I. R. McDonald, Mol. Phys. **51**, 1141 (1984).
- ³⁸ C. I. Bayly, P. Cieplak, W. D. Cornell, and P. A. Kollman, J. Phys. Chem. **97**, 10269 (1993).
- ³⁹ M. J. Frisch, G. W. Trucks, H. B. Schlegel, G. E. Scuseria, M. A. Robb, J. R. Cheeseman, V. G. Zakrzewski, J. A. Montgomery, Jr., R. E. Stratmann, J. C. Burant, et al., *Gaussian 98*, Gaussian, Inc., Pittsburgh, PA, 1998.
- ⁴⁰ P. P. Ewald, Ann. Phys. **64**, 253 (1921).
- ⁴¹ H. L. Friedman, Mol. Phys. **29**, 1533 (1975).
- ⁴² J. D. Jackson, *Classical Electrodynamics* (John Wiley & Sons, Inc., New York, 1998), 3rd ed.
- ⁴³ R. Abagyan and M. Totrov, J. Mol. Biol. **235**, 983 (1994).
- ⁴⁴ G. Petraglio, M. Ceccarelli, and M. Parrinello, J. Chem. Phys. **123**, 044103 (2005).